Validation of the Fokker-Planck analysis for NB Blip experiment on LHD

H. Nuga[1], R. Seki[1,2], S. Kamio[1], M. Osakabe[1,2], M. Yokoyama[1,2], and LHD experiment Group[1]

[1] *National Institute for Fusion Science, National Institutes of Natural Sciences, Toki, Japan*

[2] *SOKENDAI (The Graduate University for Advanced Studies), Toki, Japan*

Introduction

The behavior of beam ions on the Large Helical Device (LHD) have been analyzed by using 5 dimensional drift kinetic Monte Carlo code GNET[1]. Although the GNET code can analyze the behavior of fast ions accurately including the finite orbit width effect, it consumes a lot of computational resources and calculation time. In the view of the experimental analysis, the rapid but sufficiently accurate code which calculates the evolution of the beam momentum distribution is required. In the present research, to analyze the behavior of beam ions on LHD, we have extended three-dimensional (2D in momentum space and 1D in radial direction) Fokker-Planck (F-P) simulation code TASK/FP[2], which is a Fokker-Planck component of the integrated code TASK[3] and TASK3D-a[4]. Although Fokker-Planck codes have a difficulty to include the finite orbit width effect rather than Monte Carlo codes, it requires less computational resources and it is suitable for the analysis of a lot of experiment data.

On LHD, a series of experiments with short pulse of tangential neutral beam injection (NB-blip) have been performed[5] to investigate the confinement property of energetic particles during their slowing down processes. In the present paper, comparisons between measurements on the NB-blip experiment and our simulation results are shown.

Analysis tools

The process of our beam ion analysis consists of two steps. The first step calculates the beam birth profile using FIT3D code[6, 7]. This code inputs beam energy E_{beam}, beam port through power $P_{\mathrm{beam}}^{\mathrm{port}}$, and plasma parameters and outputs absorbed beam momentum distribution function $\partial f_b^{\mathrm{abs}}(p,\theta,\rho,t)/\partial t$, where, p, θ, and ρ denote the momentum, pitch angle, and minor radius, respectively. In this step, the prompt loss of ionized beam particle is included using orbit calculation. The second step calculates the evolution of beam momentum distribution function using TASK/FP. This code inputs $\partial f_b^{\mathrm{abs}}(p,\theta,\rho,t)/\partial t$ and plasma parameters and calculates the evolution of beam momentum distribution function.

Although TASK/FP has been developed as a full f prediction code originally, it is extended to include δf type solver to use for experimental analysis. In the present analysis, the momentum distribution function is divided into two components, $f = f_M + f_b$, where f_M and f_b denote the

momentum distribution function of bulk and beam components. The bulk component f_M is assumed to be Maxwellian with observed density $n_s(\rho,t)$ and temperature $T_s(\rho,t)$, where subscript s denotes 'species'. The evolution of f_M is not solved by using F-P equation but updated by the Maxwellian on each time step. Only beam component f_b is solved by F-P equation as below:

$$\frac{\partial f_b}{\partial t} = -\nabla_p \cdot \boldsymbol{S} + H, \tag{1}$$

where ∇_p is a derivative operator in two dimensional momentum space (p,θ) and $\boldsymbol{S}$ is a flux including collisional diffusion in the momentum space. In the present status, H term includes NB source term S_{NB}, fusion reaction source and loss term $S_{nf}(f)$, charge exchange loss term $L_{cx}(f)$, particle sink term $L_{sink}(f)$, and radial diffusion term $R(f)$, respectively. In this case, NB source term becomes $S_{NB} = \partial f_b^{\rm abs}(p,\theta,\rho,t)/\partial t$.

It is noted that the fusion reaction term and the radial diffusion term are not used in the following calculation. The density of neutral particles used for the calculation of charge exchange loss is assumed to be uniform and constant $n_{\rm neut} = 10^{15}{\rm m}^{-3}$. Additionally, an artificial particle sink term L_{sink} is used instead of the radial diffusion term to keep the total particle density near to the observed density.

NB blip experiment

Top view of NBI systems and fast ion observation system are shown in Fig. 1-(a) and 1-(b). The fast ion observation system (Si-FNA)[8] can observe the number of fast ion and its energy locally. It has four line sight and we show the analysis using one of them. Its location and pitch angle are $\rho = 0.1$ and $\theta = 163.6$ deg.

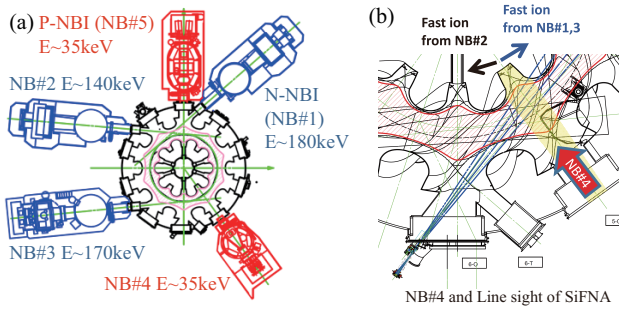

Figure 1: (a) Top view of NBI systems on LHD. NB#1 to NB#3 are tangential N-NBI and NB#4 and #5 are perpendicular P-NBI. (b) Schematic view of the fast ion measurement system.

To investigate the slowing down and the confinement of beam ions, short pulse injection of NB#2, which has a different direction to the other tangential beams, was performed. Plasma and beam ion species were hydrogen. The discharge wave form of typical NB-blip experiment is shown in Fig. 2. In the following analysis, we focus on the NB#2 injected at $t = 4.21$s until $t = 4.23$s (fig. 3). Figure 4 shows the ion momentum distribution functions in two dimensional momentum space (p,θ) at $t = 4.23$s and 4.50s. Horizontal and vertical axes denote parallel and perpendicular momentum normalized to thermal momentum.

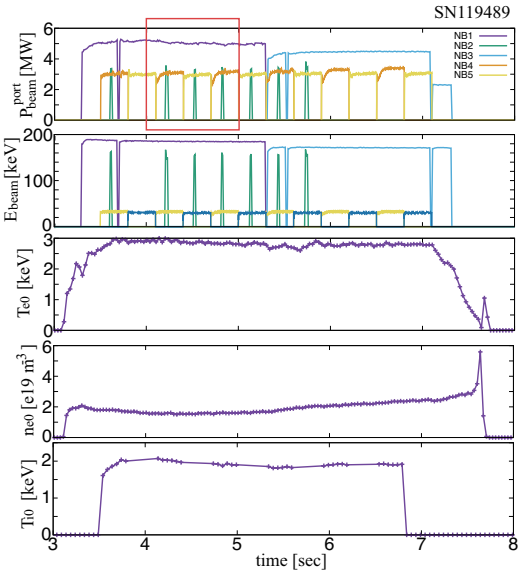

Figure 2: Discharge waveform. Evolutions of beam port through power, beam energy, electron temperature on axis, electron density on axis, and ion temperature on axis are shown.

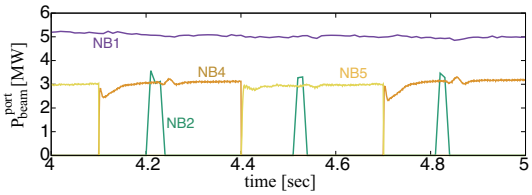

Figure 3: Beam port through power $4 < t < 5$s.

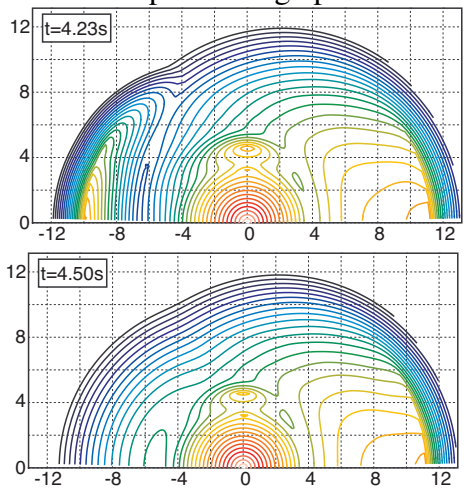

Figure 4: Momentum distribution of H ion at $t = 4.23$s and 4.50s on $\rho = 0.1$.

NB#1, 4, and 5 make steady state and their peak appear on $\theta \sim 0$ deg. and ~ 90 deg. Short pulse NB#2 appears on $\theta \sim 180$ deg. at $t = 4.23$s and the most of them are thermalized until $t = 4.50$s.

Next, comparisons between observed and simulated beam energy distribution are shown. Figure 5 shows the energy distribution of beam particles at $t = 4.24$s and 4.31s one dimensionally. Here the pitch angle and the radial position are $\theta = 163.6$ deg. and $\rho = 0.1$. It is found that the broadening of the beam component due to collisional diffusion has a good agreement. Figures 6 plot the evolutions of beam energies. This figure indicates the beam slowing down and the broadening of beam distribution between simulation and observation. The time when the beam energies reach to $\sim 50-70$ keV region has also good agreement. These results means that the collisional beam slowing down and diffusion can be solved accurately. It is noted that, In fig. 6-(b), the value of beam energy at $t = 4.21$s have more than that of the beam port through energy $E_{\mathrm{beam}} \sim 140$keV. This is because the precision of measurement is insufficient in high energy region in this fast ion observation system. Figure 7 shows the evolution of the number of beam particles in the Si-FNA line sight. The shapes between simulation and experiment are nearly same except around $t = 4.3-4.35$s. In the present simulation, the loss mechanism of beam ions

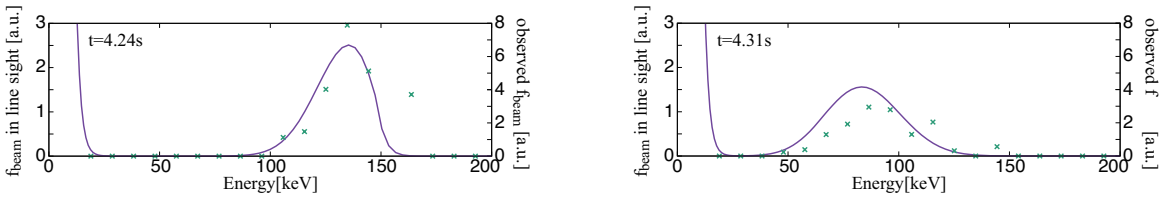

Figure 5: Energy distribution of beam particles at t = 4.24s and 4.31s. Solid curve and points denote simulation result and observed data.

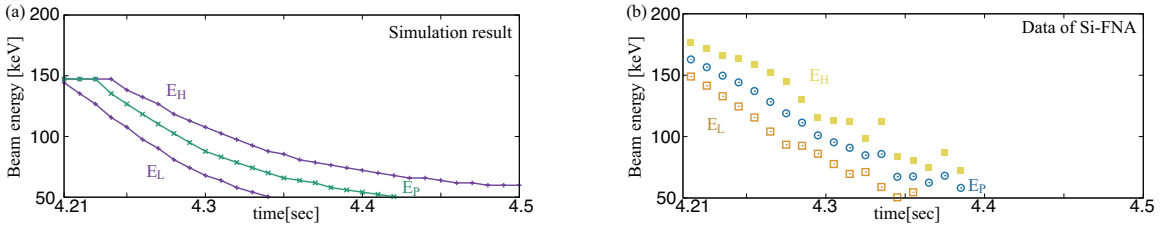

Figure 6: Evolutions of E_p, E_H, and E_L are shown. E_p is the energy of peak of f_b in θ = 163.6 deg. direction. E_L and E_H are the lower and higher energy where f_b has a half value of its peak.

are not included except for the charge exchange loss. Therefore improvement of our code to include additional loss mechanisms, such as radial transport with valid model, is required.

Conclusion

F-P code, TASK/FP, has been extended and combined to FIT3D for the analysis of beam ion. They can input measurements and output the time evolution of f_{beam}. The present analysis has a good agreement for the collisional beam slowing down and the velocity diffusion. Additionally, there is room for improvement of the beam confinement, such as a inclusion of beam transport with valid model.

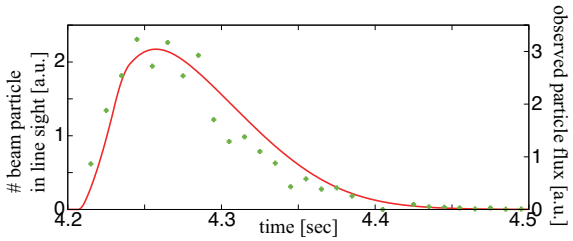

Figure 7: The evolution of the number of beam particles in the Si-FNA line sight.

References

[1] S. Murakami *et al.*, Nucl. Fusion 40, 693 (2000).

[2] H. Nuga, A. Fukuyama, Progress in NUCLEAR SCIENCE and TECHNOLOGY, **2**, 78-84, (2011).

[3] A. Fukuyama, `http://bpsi.nucleng.kyoto-u.ac.jp/task/`.

[4] M. Yokoyama, *et al*, Plasma and Fusion Research, **8**, 2403016, (2013).

[5] M. Osakabe, *et al*, Rev. Sci. Instrum. **75**, 10, (2004).

[6] S. Murakami, *et al.*, Fusion Technology, **27**, (1995).

[7] P. Vincenzi, et al, Plasma Phys. Control. Fusion, **58**, 12, 125008, (2016).

[8] M. Osakabe, *et al.*, Rev. Sci. Instrum. **72**, 788-791, (2001).